Enhanced release of palladium and platinum from catalytic converter material exposed to ammonia and chloride bearing solutions

Journal:	*Environmental Science: Processes & Impacts*
Manuscript ID	EM-ART-08-2018-000370.R2
Article Type:	Paper
Date Submitted by the Author:	06-Nov-2018
Complete List of Authors:	Aruguete, Deborah; Penn State Erie the Behrend College School of Science, Environmental Science Murayama, Mitsuhiro; Virginia Tech, Materials Science and Engineering; Virginia Tech Institute for Critical Technologies and Applied Science Blakney, Terry; Penn State Erie the Behrend College School of Science, Mathematics Winkler, Christopher; Virginia Tech, Institute for Critical Technology and Applied Science, Nanoscale Characterization and Fabrication Laboratory

Environmental Significance Statement

For “Enhanced release of palladium and platinum from catalytic converter materials exposed to ammonia and chloride bearing solutions”

Authors and affiliations:

Deborah M. Aruguete[1*], Mitsuhiro Murayama[2,3], Terry Blakney[4] and Christopher Winkler[3]

[1]Department of Environmental Science, Penn State Behrend, 4205 College Drive, Erie, PA 16563, U.S.A.
[2]Department of Materials Science and Engineering, Virginia Tech, Blacksburg, VA, 24061, U.S.A.
[3]Institute for Critical Technology and Applied Science, Nanoscale Characterization and Fabrication Laboratory, Virginia Tech, Blacksburg, VA, 24061, U.S.A
[4]Department of Mathematics, Penn State Behrend, 4205 College Drive, Erie, PA 16563

*Corresponding author: aruguete@psu.edu

Continued and increasing use of motor vehicles globally is leading to the unintentional introduction of platinum group elements (PGEs) into the environment via catalytic converter materials emitted in exhaust. Our studies suggest that palladium(Pd) and platinum(Pt) from catalytic converters can be released as coordination complexes in the presence of the environmentally-common ligands chloride and ammonia nitrogen at pH 8. Because Pd and Pt complexes with NH_3, Cl^- and similar ligands can be bioactive or toxic, our finding has strong significance as well for the impact of PGEs on ecosystems. Given the ubiquity of chloride and ammonia nitrogen, these findings may apply to a large variety of environmental systems.

Enhanced release of palladium and platinum from catalytic converter material exposed to ammonia and chloride bearing solutions

Deborah M. Aruguete[1*], *Mitsuhiro Murayama*[2,3], *Terry Blakney*[4], and *Christopher Winkler*[3]

[1]Department of Environmental Science, Penn State Behrend, 4205 College Drive, Erie, PA 16563, U.S.A.

[2]Department of Materials Science and Engineering, Virginia Tech, Blacksburg, VA, 24061, U.S.A.

[3]Institute for Critical Technology and Applied Science, Nanoscale Characterization and Fabrication Laboratory, Virginia Tech, Blacksburg, VA, 24061, U.S.A

[4]Department of Mathematics, Penn State Behrend, 4205 College Drive, Erie, PA 16563

[*]Corresponding author. E-mail address: Aruguete@psu.edu

ABSTRACT

Environmental levels of platinum group elements (PGEs) are steadily rising, primarily due to exhaust emissions of vehicle catalytic converter (VCC) materials containing solid PGEs.

Once these VCC materials reach soil and water, the PGEs may be transported in the form of nanoparticles (dimensions 1-100 nm) or they may be mobilized by forming coordination complexes with ligands in the environment. Chloride (Cl^-) and ammonia (NH_3) are two ligands of particular concern due to their ubiquity as well as their potential to form the chemotherapy drug cisplatin ($Pt(NH_3)_2Cl_2$) or other potentially bioactive complexes. This initial study examines the release of Pd and Pt into solutions exposed to VCC materials at pH 8 and 25° C, using elemental analysis of metal content in post-exposure extracts. Solutions had total ammonia nitrogen concentrations (TAN, $[NH_4^+] + [NH_3]$) of 0 μM, 5.56 μM, 55.6 μM and 1.13×10^5 μM (0 ppm, 0.1 ppm, 1 ppm, and 2147 ppm). The former three represent background environmental levels and had a minimal effect on release. However, when combined with 1.13×10^5 μM Cl^- (4000 ppm Cl^-), 55.6 μM TAN induced a marked increase in metal release (~41x for Pd). High TAN solutions induced more Pd and Pt release than equimolar NaCl solutions. Materials

characterization revealed ~4 nm palladium-containing nanoparticles were present, and spatially associated with nanoparticles of γ-Al_2O_3; ceria-zirconia nanoparticles were also present but did not have any metal associated with them. Platinum-containing nanoparticles were not observed.

I. Introduction

Platinum group elements (PGEs) are emerging pollutants of concern[1-3]. Levels of PGEs have risen since the broad institution of PGE-based vehicle catalytic converters (VCCs)[4], which convert harmful emissions to more benign gases[4, 5]. Particles of catalytic converter materials contain nanoscale (1-100 nm) and larger particles of platinum (Pt), palladium (Pd) and rhodium (Rh)[6]. These particles can be emitted with exhaust[5]. Vehicle catalytic converters are considered to be the dominant source of PGEs in the environment[3]. Platinum group elements have been found in air[7-9], roadside dust[10, 11], incinerated sewage[10] and highway tunnels[7]. Anthropogenic PGEs are even able to reach fairly pristine systems as demonstrated by their discovery in Antarctic ice[12]. PGE emissions are expected to increase as automobile sales grow.

Vehicle sales and registrations have risen from approximately 66 million vehicles in 2005 to 97 million in 2017, a 46% increase overall[13] 1,282,270 vehicles are in use as of 2015, including passenger and commercial vehicles.[14] In developing countries, sales have risen sharply, leading to concerns about PGE pollution in these areas[15]. For example, from 2005 to 2012 sales in China rose from 5.7 million to 29 million[13]. Recently tightened emissions regulations in the EU and US[16] have led to an increased loading of Pd in VCCs, indicating that overall Pd emissions into the environment may increase.

This increase is of concern because PGE materials in the environment could damage human and ecosystem health. Negative impacts could arise if VCC-based PGE metals could be transformed into bioactive PGE coordination complexes such as the chemotherapy drug cisplatin[17] ($Pt(NH_3)_2Cl_2$) or other PGE compounds of pharmaceutical interest[18-20]. Whereas such substances are useful in medicine, their uncontrolled introduction into the environment may be problematic as they can be detrimental to microbes[21-23] and larger organisms[19, 23]. Negative impacts could also arise even if the PGEs remain unchanged because they are nanoparticles (particles with dimensions of 1-100 nm)[6, 24]. Nanoparticles frequently display size-dependent chemical properties different from those of bulk counterparts such as redox potential, solubility, and surface energy, making them more reactive and often more toxic than their bulk counterparts[25, 26]. VCC materials in particular have been noted as a critical part of outdoor urban nanomaterials[27].

As of now, predicting the fate of VCC PGE nanoparticles is difficult. Regardless, it is clear that compounds present in the environment can increase the release of Pd and Pt from solid VCC materials into solution. These compounds include methionine[28], citric acid[28], and humic acids[29], as well as the anions NO_3^-, SO_4^{2-}, Cl^- and PO_4^{3-}[30-32]. Pd and Pt release from VCC materials has also been observed in simulated biological fluids with chloride[8, 33].

In such systems, at least in part, the release of Pd and Pt into solution from VCC materials likely entails a process involving the dissolution of oxidized species on the metal particles coupled with the formation of coordination complexes. Even under ambient conditions[34], native surface oxides or oxidized surfaces with adsorbed oxygen can exist on Pd[28] and Pt[34] with thicknesses ranging from <1 to ~10 monolayers[35]. A divalent oxidation state of the surface layer is most likely to be favored at these experimental conditions for Pd[36] and Pt[37-40]. Dissolution of this oxidized surface can occur as per equation 1[41] (for ease of presentation $(Pd/Pt)(OH)_2(s)$ is used to represent the surface oxide material based on prior work on Pd[41], although many oxide stoichiometries are possible). This reaction can be coupled with the formation of a Pd or Pt complex with the ligand X, shown in equation 2[42]. If the complexation is highly favored, it can thermodynamically drive the release of Pd and Pt into solution. An energetically favorable ligand exchange of a non-water ligand Y for X[43] (equation 3) can drive these coupled processes farther to the right. For all reactions, m is the number of ligands in the complex (l = 0, 1, 2, 3, 4) with a charge q.

$(Pd/Pt)(OH)_2(s) + 2H^+(aq) + 2H_2O(l) \rightarrow (Pd/Pt)(H_2O)_4^{2+}(aq)$ dissolution (1)

$(Pd/Pt)(H_2O)_4^{2+}(aq) + mX^q(aq) \rightarrow (Pd/Pt)(X)_m(H_2O)_{4-m}^{2+m\times q}(aq) + mH_2O(l)$ complex formation(2)

$(Pd/Pt)(X)_m(H_2O)_{4-m}^{2+m\times q}(aq) + Y(aq) \rightarrow (Pd/Pt)(X)_{m-1}(Y)(H_2O)_{3-m}^{2+(m-1)q}(aq) + X^m$ ligand exchange (3)

Thus, in considering the solubility of solid Pd and Pt, ligands that are (i) extremely common in the environment and (ii) form highly stable Pd and Pt coordination complexes are of particular interest, as they may increase solubility. The ligands chloride (Cl^-) and ammonia (NH_3) were chosen for these reasons.

Chloride (Cl^-) and ammonia (NH_3) form highly stable coordination complexes with PGEs, particularly Pd and Pt, as indicated by cumulative stability constant (β_4) values[44-46]. The affinity of Cl^- and NH_3 for Pd and Pt is such that they are even used in ore refinement[47-49]. Most notably, at environmentally-relevant concentrations of NH_3 and Cl^- similar to this study, Eh-pH calculations indicate that mixed-ligand complexes such as $Pd(NH_3)Cl^+$ are energetically favored at pH 6-8 and a wide range of oxidation potentials[39].

In addition to equilibrium chemistry, understanding Pd and Pt interactions with Cl^- and NH_3 is critical as both of these ligands are ubiquitous in natural systems, and frequently elevated in polluted systems. At common environmental pH values, NH_3 exists with NH_4^+ (ammonium) as a conjugate base-weak acid pair. With increasing pH, the proportion of NH_3 relative to NH_4^+ will increase (pK_a of $NH_4^+ = 9.4$ at 20°C)[50], making this ligand particularly important for PGE complexation under mildly basic pH conditions, as opposed to pH values < 7. Ammonia (NH_3) and ammonium (NH_4^+) are collectively referred to as ammonia nitrogen (AN)‡. Natural sources of AN include soil microbial activity[51] and decay of natural organic matter[52]. Human activity can also contribute to excess AN levels, from sources such as ammonia fertilizer[53], wastewater[53] and emissions from burning coal[51]. Once introduced into the environment, AN is often oxidized due to processes such as nitrification. Soil has background levels of 55.6 μM M to 278 μM total ammonia nitrogen (TAN, defined[53] as $[NH_4^+] + [NH_3]$)‡ and < 333 μM in surface freshwater, but can be >1.7 × 10^5 μM temporarily after fertilizer application[52]. Understanding how AN affects Pd and Pt release into solution is relevant for any similar or related amine species in the environment, *e.g.* amino acids[54].

Chloride is naturally present in soil, freshwater, and of course marine systems. Chloride levels are rising to excess in many terrestrial systems due to human activity. Anthropogenic sources include salt buildup in heavily irrigated fields[55, 56], road de-icing salt[57-59], and landfill leachate[60]. With sea level rise, ocean incursion has increased the salinity of many coastal areas [61, 62]. Unlike AN, chloride is persistent and can readily accumulate in the environment. Continually rising chloride in the environment could potentially increase the release of Pd and Pt into solution due to the formation of chloro-Pd or -Pt complexes.

The overall purpose of this study is to determine the effects of ammonia nitrogen and chloride upon the release of Pd and Pt from VCC materials at ambient conditions (pH 8, 20°C) using batch-mixing trials. Specifically, the first aim is to determine the effect of ammonia nitrogen concentration upon metal release into solution, both at realistic background levels found in soil solution and water[52, 53] (0 μM, 5.56 μM, 55.6 μM and 1.13×10^5 μM) as well as an elevated post-fertilization level (1.13×10^5 μM TAN). The second aim is to determine the effect of elevated salinity (as NaCl) upon metal release, using a concentration of 1.13×10^5 μM Cl^-, representative of salt levels in snow and water contaminated with road salt[58, 63] as well as brackish or estuarine waters[64]. The third is to examine how mixed solutions with both elevated chloride and the TAN levels above impact metal release. The fourth aim was to explore how nanoparticulate components (dimensions < 100 nm) of VCC materials might impact Pd and Pt release. To this end, two specific goals were to perform a thorough materials characterization, and to elucidate whether released Pd and Pt could be in the form of colloidal nanoparticles rather than metal coordination complexes.

II. Materials and methods

A commercially-available unused vehicle catalytic converter for the 2007 and 2008 Honda Fit base models (economy cars, Honda OEM Part No. 18160-RME-A00) was used for this study. This VCC is for gasoline engines. The catalytic converter chassis was cut open to reveal two monoliths. For consistency, only the first monolith (what would be closest to the engine) was used. The monolith was placed into new zipper-locked plastic bags and gently tapped with a plastic hammer to break it apart. The pieces were then ground to a powder with an agate mortar and pestle, and subsequently stored sealed in the dark. Laboratory chemicals used, namely NH_4Cl, NH_4NO_3, $NaNO_3$ and NaC, were all Reagent Grade purity or higher and purchased from Sigma-Aldrich. Ultrapure (18.2 MΩ-cm) water was used for all solutions, and Fisher TraceMetal nitric acid for sample acidification.

Batch solubility experiments were conducted with solutions serving as simplified models of environmental waters, including those polluted with excess AN or salt. 0.500

g of VCC powder were weighed into an acid-washed borosilicate glass vial along with 20 mL of solution, capped and magnetically stirred for 48 hours at room temperature. They were kept in the dark to eliminate any possible photochemistry. pH was measured in solutions before and after the experiments and found to be constant within 0.2 pH units.

1.13×10^5 μM Cl^- (4000 ppm Cl^-) solutions representing salt-polluted water[58, 63, 64] were prepared with NaCl and are designated as “Cl-only.” 0.113 M $NaNO_3$ solutions were prepared as the control. Ammonia nitrogen solutions were prepared with NH_4NO_3 at concentrations representative of background levels in the environment[52] of 0 M, 5.56 μM, and 55.6 μM corresponding to 0 ppm, 0.1 ppm, and 1 ppm TAN. These concentrations were all less than the EPA designated Chronic Criterion Magnitude limit of 150 μM TAN (2.7 ppm) at 20 °C and pH 8. A 1.13×10^5 μM NH_4NO_3 solution was also made to represent soils immediately after fertilization[52]. Sodium nitrate ($NaNO_3$) was added to the low TAN solutions to maintain constant ionic strength. These solutions are referred to as “low TAN-only”, “mid TAN-only” and “high TAN-only” in the remainder of the text. An additional series of solutions with the same TAN levels was prepared with NaCl at a concentration of 1.13×10^5 µM. These are designated as "low TAN-Cl" and so forth. All solutions were adjusted to pH 8 with $NaHCO_3$ (1000 µM in final solutions) except for the high TAN and high TAN-Cl solutions, which were adjusted with NaOH as AN acted as a buffer. After stirring, the VCC-solution mixture was decanted and filtered through a 0.2 µm PVDF syringe filter (Millipore). This filtered extract was then acidified to 2-5% HNO_3 by volume, weighed, and stored in LDPE bottles at 4° C prior to elemental analysis. A minimum of five reagent blank[65] trials were run at the same time as the standard experiments. These blanks were analyzed to quantify any contamination introduced during the experiments and sample processing.

To assess extracts for the presence of particles <0.2 µm, a portion was subjected to centrifugal ultrafiltration through a 1 kilodalton molecular weight cutoff filter (Pall Macrosep Advance Centrifugal Filter, ~1.4 nm pore size[66]), then analyzing the filtrate and retentate separately. Another portion was also ultracentrifuged at 75000 rpm with a Beckman Optima TL ultracentrifuge, and the top and bottom fractions subjected to elemental analysis. Further details of these experiments are provided in section V of the ESI.

Elemental analysis of extracts for Pd, Pt and Rh was performed at the Penn State Laboratory for Isotopes and Metals in the Environment (LIME), using a ThermoX Series II Quadrupole Inductively Coupled Plasma Mass Spectrometer (ICP-MS) with collision cell technology. A list of the operating parameters for the instrument (*e.g.* gas flow rates) is provided in Table S4 of the ESI (Part II, page S4). Data was analyzed to account for common expected interferences from polyatomic species formed with the metals Cu, Zn, Sr, Rb, Y, Zr, Mo, Gd, Hf, Ta, Pb as well as Cd isotopes isobaric with Pd isotopes. Table S5 in the ESI lists some of the more common mass interferences.

To be considered a significant mass interference requiring correction, the signal counts at the atomic mass numbers of interfering elements had to be >5% of the putative Pd or Pt signal and have isotopic ratios consistent with natural abundances. As these samples were generated from simplified, controlled experiments, they were mostly not expected to contain any significant amount of elements causing mass interferences. In accordance, it was found that isotopes 176-180 of Hf had concentrations below detection limits, as well as Y, Zr, Nb, Ta and Cd. The only significant contaminant was Sr. Aside from high TAN solutions, all other measurements were indistinguishable from reagent blanks, as confirmed by the statistical analysis (described here and in section III of the ESI). The instrumental detection limits reported by the LIME facility were 18.8 μM for Pd, 10.2 μM for Pt and 29.1 μM for Rh. Limits of detection (LODs) were calculated as $X_{\text{blank}} + 3\,\sigma_{\text{blank}}$, with X_{blank} being the average value of the blank samples and σ_{blank} being the standard deviation for these samples[67].

Statistical analysis. To assess the statistical significance (95% Confidence Intervals) of differences in Pd and Pt content between varying solution compositions, data were subjected to the Andersen-Darling Test for Normality ($\alpha = 0.05$) and subsequently analyzed with two sample t-tests in cases of normally distributed data or Mann-Whitney tests if the normality assumption

was violated. When comparing more than two samples the Mood's Median test was employed when the normality assumption was violated by at least one of the three samples tested. Otherwise, ANOVA combined with Tukey's test for pairwise comparison were employed. Analysis was performed using the MINITAB software package. Further information on the analysis is provided in the ESI.

Characterization of VCC materials. Elemental analysis of the whole solid catalytic converter material as well as NIST SRM 2557 (Used Autocatalyst) was performed by Activation Laboratories Ltd. (Ancaster, ON, Canada; www.actlabs.com), report A16-05871. Platinum, palladium and gold were extracted via fire assay and analyzed by ICP-OES. Rh was extracted by fire assay and analyzed with ICP-MS. To extract Zr and Ce, fusion with lithium metaborate tetraborate was performed and analysis done with ICP-OES/MS. (Actlabs codes for tests: 1C – OES, 1C –Rhodium, 4Litho.)

Material collected for electron microscopy characterization was obtained by gently scraping surfaces of the CC monolith. This was done in order to limit sampling to the active catalytic material, as opposed to the underlying support (cordierite). Subsequently the scrapings were suspended in hexanes, deposited on a Cu-ultrathin carbon film grid (Electron Microscopy Sciences) and allowed to dry. Conventional diffraction-contrast images, selected area electron diffraction (SAED), and elemental maps from energy-dispersive X-rays (EDX) were collected using a JEOL JEM-2100 transmission electron microscope (TEM) equipped with a JEOL genuine 60mm^2 Silicon Drift detector (SDD) EDX system operating at 200 kV. Site-specific EDX analysis was performed using a high intensity electron probe (resolution < 1 nm) in an FEI Titan 80-300 field emission TEM operating at 300 kV. This instrument was equipped with a Fischione high angle annular dark field (HAADF) detector to obtain Z (atomic number) - contrast images in scanning transmission electron microscopy (STEM) mode and an EDAX 30 mm^2 Si(Li) EDX system. High-resolution transmission electron microscopy (HRTEM) images and corresponding Fast Fourier Transform (FFT) patterns were analyzed for crystalline phases, using Gatan DigitalMicrograph and FEI TIA software. The American Mineralogist Crystal Structures Database was referenced for this analysis. In addition to TEM and EDX work, powder X-ray diffraction (XRD) data were collected from the whole VCC material using a Rigaku Mini-Flex diffractomer with Cu-Kα radiation. Brunauer-Emmett-Teller (BET) surface area analysis of the powder was performed with a Quantachrome AS1 BET analyzer.

III. Results and Discussion

1. Bulk analyses of whole VCC monolith materials. In the elemental analysis of the whole VCC material, palladium, platinum and rhodium were all found to be present, with palladium present at the highest concentration. Table 1 lists the results of these analyses. The molar ratio of palladium to platinum was ~21:1 and palladium to rhodium was ~11:1. Zirconium and cerium are present, with a molar ratio of Zr:Ce equal to ~5.25:1. Powder XRD (ESI figure S1) confirmed the presence of cordierite ($(Mg,Fe)_2Al_3(Si_5AlO_{18})$), which was to be expected as cordierite is the dominant material within a monolith, serving as the substrate for catalytic materials. The BET surface area of the powder was 54.2 m^2/g. The XRD and BET observations are not surprising, because the whole solid was analyzed as opposed materials on the monolith surface, which are dominated by washcoat and catalyst nanomaterials.

2. TEM and SAED analysis of oxide washcoat. Conventional TEM images of materials scraped from the monolith surface are displayed in figure 1A, displaying clusters of rounded, slightly elliptical structures ~10-15 nm in diameter (figure 1B) and lathe-like structures <5 nm thick (figure 1C), referred to as nanodots and nanoflakes. Selected area electron diffraction (SAED) of the Zr-Ce nanodots (Figure 1D) was consistent with ceria-zirconia[68]. Selected area electron diffraction (SAED) of the nanoflakes (Figure 1E) was consistent with that of γ -Al_2O_3 [69]. SAED indexing is provided in ESI Tables S1 and S2. Figure 2 displays representative results from elemental mapping via energy dispersive x-ray spectroscopy (EDS). Areas with lathe-like structures had a high aluminum content, whereas the rounded structures displayed a high zirconium content, along with a small amount of cerium. The Zr and Ce maps are thus consistent with the elemental analysis of the whole powder VCC material.

3. Localized spectroscopic analysis and HRTEM of Pd-rich areas. Energy-dispersive X-ray (EDX) spectroscopy and STEM-HAADF were employed to obtain highly-localized chemical information. The contrast in HAADF imaging is proportional to Z^2 (atomic mass squared). This is evident in figure 3A, which is a HAADF-STEM image of the rightmost structure in figure 1A. This structure is a mass of γ-Al_2O_3 nanoflakes and ceria-zirconia nanodots; the higher-Z nanodots have a much stronger contrast. A magnified part of the structure in Figure 3A is shown in Figure 3B with two points from which spectra were collected. These spectra are representative of those collected from other areas. Point 1 corresponds to a lower-contrast area of γ-Al_2O_3, while point 2 corresponds to a higher-contrast ceria-zirconia nanodot. In figure 3C, EDX spectra are shown for point 1 and point 2. Point 1 was collected from γ-Al_2O_3 nanoflakes, and displays emission consistent with palladium Lα at 2.838 keV, as well as a signal consistent with an Al-Al sum peak, marked with an asterisk in Figure 3C. Point 2 displays a cerium and zirconium signal consistent with ceria-zirconia. Notably, there is no Pd signal associated with the Ce and Zr signals. In any of the areas analyzed, the presence or absence of Pt cannot be confirmed, as the characteristic M peak of Pt (2.048 keV) overlaps with the Lα peak for Zr (2.042 keV) and no Pt Lα signal is present. No Rh Lα peak (2.696 keV) was observed in any areas sampled. This is consistent with the elemental analysis of the solid, which showed that the Pd content was greater than that of Pt or Rh. Also, very importantly, sampling is limited compared to ensemble characterization techniques. The additional elements in the EDX spectra can be readily attributed to other known sources. Copper and carbon are likely from the substrate used (copper grid with carbon film). Some of the underlying cordierite material was likely picked up as part of the VCC scrapings, explaining the Si signal. High resolution TEM imaging was then performed on spot 1. Particles distinct from the γ-Al_2O_3

nanoflakes were found and shown in Figures 3D1 and 3D2. In all imaging, these particles were only observed when EDX spectra indicated the presence of palladium. Fast Fourier Transform (FFT) images from Figure 3D1 and 3D2 indicate a possible presence of palladium oxide, although it is not definitive (see page 2 of ESI regarding analysis). The presence of oxidized Pd is consistent with other work in which via X-ray absorption spectroscopy of Pt in VCC materials revealed Pt oxidic species[6]. Surface-enhanced Raman spectroscopy (SERS) on PGE surfaces indicates that oxide species can form even under mild conditions[35]. The presence of non-metallic Pd even prior to solution exposure could indicate that Pd metal oxidation (equation 1) is not significant for the chemistry of Pd release into solution, but rather dissolution, complexation, and ligand exchange (equations 1-4).

4. Release of Pd and Pt into solution. Palladium and platinum concentrations in extracts from VCCs are presented in Figures 4A and 4B respectively. Average concentrations of Pd and Pt in extracts are provided in Tables 2 and 3. Palladium was more soluble than platinum, consistent with what is generally known about their relative reactivity[36].

Palladium and platinum displayed similar trends in solution release with respect to AN and Cl^- content. Far less platinum was extracted into solutions than palladium, even though stability constants for ammino-Pt and chloro-Pt complexes are greater than their Pd counterparts. The lower Pt levels may be linked to the energetics of their oxidations; log $K_{Pdox}°$ is ~ -30[44] whereas log $K_{Ptox}°$ is ~ -41[70]. Also, there is a large discrepancy in the complexation kinetics, with Pd complex formation being ~10^4-10^5 times faster than Pt[71].

Results and analysis from the ultracentrifugation and ultrafiltration of high TAN-Cl extracts are presented in Section IV of the ESI. Ultracentrifugation and subsequent analysis of the top and bottom fractions from centrifuge tubes revealed no significant difference. The minimum size of particle that could be moved to the bottom is ~2.4 nm. Analysis of the retentate and ultrafiltrate from ultrafiltration did not show any difference in concentration. The approximate pore size is ~1.5 nm. These results indicate that any nanoparticles contributing to the Pd and Pt signal would have to be smaller than 1.5 – 2 nm. The observed Pd nanoparticles in the VCC material had dimensions of ~4 nm. Additionally, a recent study indicates that platinum extracted from a sonicated road dust leachate is in the form of nanoparticles with dimensions of 9 - 21 nm[72]. Based on these factors, it is arguably unlikely that nanoparticles are contributing in any substantial way to the Pd and Pt content of the extracts.

5. Effect of AN-only and chloride-only solutions on Pd and Pt release. Both Cl-only solutions (1.13×10^5 µM) and equimolar high TAN-only solutions increased the release of Pd and Pt relative to control solutions of 1.13×10^5 µM $NaNO_3$. Ammonia nitrogen had a greater effect than Cl^-. The average [Pd] in high TAN-only solutions was 54.9 µM (±9.1), ~229 times greater than the 0.24 µM (±0.04) found in Cl-only extracts. For Pt solutions, the average [Pt] in high TAN-only extracts was 0.0079 µM (±0.0036), ~16 times greater than the 4.8×10^{-4} µM ($\pm 1.3 \times 10^{-4}$ µM) in Cl-only extracts. It is to be noted that only ~5.6% of the TAN is NH_3(6320 × µM M), assuming a K_a value of 5.6×10^{-10} at 25 °C for NH_4^+.)[50])

6. Pd and Pt release into AN-only solutions vs. AN-Cl^- solutions. The release of Pd and Pt in AN-Cl^- solutions was often greater than that in AN-only solutions. Interestingly, the mixture of both ligands often induced a synergistic effect, increasing Pd and Pt release to a greater degree than both AN-only and Cl-only solutions combined. This was demonstrated for Pd in mid TAN-Cl and high-TAN-Cl solutions. The mid TAN-Cl extracts had an average [Pd] of 2.41 μM (±1.22) , a ~41-fold increase from the corresponding AN-only extracts at 0.059 μM (±0.040). The combined [Pd] from Cl-only and mid TAN-only extracts is 0.299 μM (±0.058), markedly lower than [Pd] in the mixed ligand extracts. As for high TAN, the high TAN-Cl- extracts had an average [Pd] of 75.5 μM (±14.7), a ~1.4-fold increase from the corresponding high TAN-only extracts at 54.8 μM (±9.1). The combined average [Pd] of high TAN-only and Cl-only extracts were 55.1 μM Pd (±9.1)), significantly less than the average [Pd] in the high TAN-Cl extracts.

Platinum release also displayed a synergistic increase in mid TAN-Cl extracts. The average [Pt] in mid TAN-Cl was 0.001 μM (±0.0001). This cannot be attributed solely to chloride, as the Cl-only solutions had an average [Pt] of 1.9×10^{-4} μM ($\pm 1.2 \times 10^{-4}$) nor can it be attributed solely to AN as the average [Pt] in mid TAN-only solutions was 2.4×10^{-4} μM ($\pm 0.7 \times 10^{-4}$) (indistinguishable from levels in reagent blank). On the other hand, for high TAN solutions, there was no difference in Pt levels between high TAN-only and high TAN-Cl extracts.

For both Pd and Pt, low TAN solutions were not distinguishable from controls. VCC-PGEs exposed to low TAN-Cl solutions released a greater amount of Pd and Pt into solution, but it was not distinguishable from the solubility in Cl-only solutions. Thus, no synergistic effects were detectable in these mixtures.

7. Simplified coordination chemistry model and trends in PGE release.

The observed dependencies of Pd and Pt release from the VCC material are consistent with calculated and empirically determined speciation studies performed at conditions relevant to this study. Colombo and co-workers[39] examined the impact of NH_3 and Cl^- at conditions relevant to this study (Σ[N] = 0.5 μM, Σ[Cl] = 0 μM, 25° C) by constructing Eh-pH diagrams with the HSC Chemistry model. Of note is that Pd solubility was predicted at Eh = 0.4 – 0.8 eV for a broad range of pH values (0-8), with speciation dominated be $PdCl_4^{2-}$ at acid pH and progressing towards complexes with NH_3 and OH^- ligands as pH increased. At pH 8, the predicted species was $Pd(NH_3)_3Cl^+$. In the absence of Cl^-, in the same E_h range, the predicted species was $Pd(NH_3)_4^{2+}$. Both with and without Cl^-, at the same concentration of N, Pt was soluble in the form $Pt(NH_3)_4^{2+}$, but with a more limited Eh range (0.6 – 0.8 eV). Calculations by Wood and co-workers[38, 73] have predicted complexation of Pt and Pd with Cl^- and NH_3. In one study, he examined Pd speciation as a function of the activities of NH_3 and Cl^{-} at 25° C. At $\log a_{Cl^-} \sim -1$, and $\log a_{NH_3} = -9$ to -5, Pd-Cl-NH_3 complexes are predicted to dominate.

Empirical measurements have also shed insight onto what complexes are actually present. Cosden and Byrne[74], for example, used UV absorption spectroscopy to identify species in systems relevant to seawater and estuarine water. At pH ~8 and $[Cl^-] \sim 5.56 \times 10^5$ μM (seawater concentration), $PdCl_3OH$ and $PtCl_3OH$ were observed to dominate. Van Middlesworth and Wood[41] examined the solubility of $Pd(OH)_2$, a disordered hydroxide (akin potentially to disordered oxidized layer on Pd nanoparticles) from pH 0-12, varying $[Cl^-]$ from 0 M to 1 M. They fit an equilibrium model to their specific results and derived that three aqueous species dominated: $PdCl_4^{2-}$, $PdCl_2(OH)_2^{2-}$, and $Pd(OH)_2^0$ (the latter dominated in conditions similar to those of this study). UV-visible spectroscopic measurements of Pd(II) and Pt(II) complexes with ligands Cl^-, OH^-, NH_3 and H_2O are well-known from past work, with Reinhardt[75-78] and Elding[46, 79-90] leading some of the earliest studies.

Based upon this body of theoretical and empirical studies, a simplified Pd(II) and Pt(II) coordination chemistry framework solely involving the ligands Cl^-, H_2O, and NH_3 is provided here to conceptually describe the release of Pd and Pt from the VCC material. For simplicity

ligands such as OH^- and CO_3^{2-} [41, 91 74] are excluded. The reactions discussed below are not intended to be a comprehensive account of all chemical processes, but rather to provide a useful qualitative model.

7. Effect of single ligand solutions (Cl-only and AN-only solutions) on PGE release.

For the single ligand solutions in this model, the following two complexation reactions starting with a tetraaqua-palladate[76, 82] or -platinate[73, 85, 88] are considered, namely the formation of chloro(aqua)-palladates and –platinates,

$$(Pd/Pt)(H_2O)_4^{2+}(aq) + mCl^-(aq) \rightarrow (Pd/Pt)(Cl)_m(H_2O)_{4-m}^{2-m}(aq) + mH_2O$$

(4)

and the formation of ammino(aqua)-palladates and –platinates in AN-only solutions,

$$(Pd/Pt)(H_2O)_4^{2+}(aq) + nNH_3(aq) \rightarrow (Pd/Pt)(NH_3)_n(H_2O)_{4-n}^{2+}(aq) + nH_2O$$

(5)

where *m* and *n* are integers with values of 0, 1, 2, 3, or 4, and the coordination number of PGE(II) limited to four.

Chloride-only solutions and the equimolar high TAN-only solutions both increased Pd and Pt release relative to controls. The high TAN-only solution induced significantly more release than the Cl-only solution, despite the fact that only 5.6% of the AN is in the NH_3 form ($[NH_3]$ = 633 μM). This is unsurprising, as the formation of ammino-PGE complexes is far more energetically favored than the formation of chloro-PGE complexes. This is evident upon examination of cumulative stability constants for equations 4 and 5. Log β_4 values for complex formation are 32.8 for $Pd(NH_3)_4^{2+}$, 35.5 for $Pt(NH_3)_4^{2+}$, 13.1 for $PdCl_4^{2-}$, and 15 for $PtCl_4^{2-}$.[44, 73, 76, 89] Further information on stepwise stability constants is provided in ESI section V.

Release of PGE into solution decreases as TAN decreases, but the relationship is not directly proportional. This is consistent with the equilibrium expression for equation 5 for which β_m is the cumulative stability constant:

$$\beta_m = \frac{[(\mathrm{Pd/Pt})(NH_3)_m(H_2O)_{4-m}{}^{2+}]}{[(\mathrm{Pd/Pt})(H_2O)_4{}^{2+}]\,[NH_3]^m} \qquad (6)$$

For $n > 1$, $\left[(\mathrm{Pd/Pt})(\mathrm{NH_3})_m(\mathrm{H_2O})_{4-m}{}^{2+}\right]$ has a non-linear dependence on $[NH_3]$.

Effect of mixed ligand solutions (AN and Cl-) on Pd and Pt release.

The kinetics of complexation and ligand exchange may provide insight into the behavior of Pd and Pt when exposed to mixtures of ligands. This can be based upon the interaction of the ligand with Pd^{2+} and Pt^{2+}, as complexation rates can vary depending upon the ligand[46, 76-78, 81, 82, 85, 87, 90]. Another factor that can alter the kinetics is the concentration of the respective ligands. To understand the possible interplay between these two factors, the first complexation step is considered (equation 7)

$$(\mathrm{Pd/Pt})(\mathrm{H_2O})_4^{2+} + \mathrm{X}^{i} \rightarrow (\mathrm{Pd/Pt})(\mathrm{H_2O})_3\mathrm{X}^{2-i} + \mathrm{H_2O} \qquad (7)$$

where X = Cl^- or NH_3.

If X is in sufficient excess, the forward reaction obeys a pseudo first-order rate law as follows[43]:

$$\text{rate} = (k_{-1} + k_1[\mathrm{X}])[(\mathrm{Pd/Pt})(\mathrm{H_2O})_4^{2+}] \qquad (8)$$

where k_1 is the rate constant for the forward reaction and k_{-1} the rate constant for the reverse reaction. (Literature values of rate constants for Pd and Pt are provided in

Section V of the ESI for the convenience of the reader.) Assuming trends similar to those under comparable experimental conditions, the rate constant for the first complexation step with Cl^-, namely $k_1(Cl^-)$, is equal to 1.8 × 10^4 s^{-1} M^{-l}. The constant $k_1(NH_3)$ is equal to 8.0 × 10^4 s^{-1} M^{-l}, on the same order of magnitude as $k_1(Cl^-)$. The reverse reaction constants $k_{-1} << k_1$, with $k_{-1}(Cl^-) = 0.83\ s^{-1}$ and $k_{-1}(Cl^-) \sim 2 \times 10^{-5}\ s^{-1}$.[92] Thus, when $[Cl^-] >>[NH_3]$, it is likely that $(Pd/Pt)(H_2O)_3Cl^+$ (and other chloro aqua species) forms at a faster rate than $(Pd/Pt)(H_2O)_3NH_3^{2+}$.

Subsequently, $(Pd/Pt)(Cl)_i(H_2O)_{4-i}^{2-i}$ complexes could undergo ligand exchange for NH_3:

$$(Pd/Pt)(Cl)_i(H_2O)_{4-i}^{2-i}(aq) + NH_3(aq) \rightarrow (Pd/Pt)(Cl)_{i-1}(NH_3)(H_2O)_{4-i}^{2-i}(aq) + Cl^-(aq) \quad (9)$$

The exchange of Cl^- for NH_3 is very energetically favored (*e.g.* log K ≥ 4.2 for stepwise substitution of $PdCl_4^{2-} \rightarrow Pd(NH_3)_4^{2+}$)[75, 77].

An interesting feature of the synergistic effect in our studies is that it was greatest in mid TAN-Cl solutions (~41-fold for Pd) and limited (or not detected) for high TAN-Cl solutions (~1.4-fold for Pd). As noted above, ammino-Pd or -Pt complex formation at low $[NH_3]$ is reduced and slowed relative to chloro-Pd or -Pt complexes solely due to the limited concentration, not because of intrinsically being kinetically or thermodynamically favored. In this case, as direct formation of ammino-Pd or -Pt complexes (equation 5) is very limited, the additional possible reactions (equations 5 and 10) introduced can have a significant effect. Increasing [NH_3] will increase the direct formation of ammino-Pd or -Pt complexes, which makes the relative “advantage” conferred by Cl^- less significant.

The low TAN-Cl solutions demonstrated no synergistic effect on Pd or Pt release, in spite of the pronounced effect in the mid TAN-Cl solutions. This behavior is a useful indicator regarding the limitations of the simplified model. For example, the rate law in equation 8 may not apply at low [NH_3], as it is only valid when the ligand [X] is in sufficient excess of [$(Pd/Pt)(H_2O)_4^{2+}$][43]. The simplified model only concerns aqueous chemistry, neglecting anything about processes on particle surfaces.

Conclusion

In summary, ammonia nitrogen (AN) and chloride (Cl^-) can induce the release of VCC-based Pd and Pt into a mildly basic solution (pH 8) under ambient conditions. Pd release was greater than Pt release. Palladium and platinum release in AN solutions was minimal or undetectable at typical background levels of AN in soil and water (0 µM, 5.56 μM, 55.6 μM), but significantly increased at an elevated TAN level representative of recently-fertilized systems (119.2 μM). Chloride solutions (1.13×10^5 μM Cl^- as NaCl) representing salt polluted or brackish systems increased Pd and Pt release, with equimolar AN solutions induced up to ~229 times more release. Most interestingly, a synergistic (non-additive) effect upon metal release is observed when VCC materials are exposed to both ligands simultaneously. Exposing VCC materials to mixed ligand solutions with both 1.13×10^5 μM Cl^- and AN increased metal release, especially at mid TAN levels. This result implies that even at trace levels in a system, ammonia nitrogen and related substances may be transformed from something relatively innocuous to potent metal mobilizers, simply by introducing Cl^-. Materials characterization indicated that palladium, likely in an oxidic form, was present as ~4 nm nanoparticles associated with γ-Al_2O_3 nanoparticles but not with $Ce_xZr_{1-x}O_2$ nanoparticles.

It is notable that even for complex, heterogeneous, nanoscale VCC materials, very basic knowledge of the stability constants and kinetics of Pd and Pt coordination complex processes could qualitatively predict most of the behavior observed. Even though ultrafiltration and ultracentrifugation results did not rule out the presence of Pd-or Pt-bearing colloids <1-2 nm, the predictive utility of complexation chemistry implies that it is playing a dominant role in Pd and Pt release from solid materials.

This initial work can form the basis for several future studies. These include a closer investigation of complexation chemistry on Pd and Pt mobilization, including increased understanding of the role of ligand exchange kinetics. The materials characterization can be used as a basis for selecting model compounds for further study to connect chemical behavior to materials size, shape, and spatial association. Comparing the behavior of the fresh catalytic converter in this study to used catalytic converter (same model) will also be essential in understanding the environmental fate of VCC material in various stages of use. Additionally, given its pronounced lability, palladium may affect the environment more than other PGEs, indicating that it merits further intensive study.

Conflicts of interest

There are no conflicts to declare.

Acknowledgements

This project was supported by Penn State Behrend startup funds (DMA), the Virginia Tech National Center for Earth and Environmental Nanotechnology Infrastructure (NanoEarth), a member of the National Nanotechnology Coordinated Infrastructure (NNCI), supported by NSF (ECCS 1542100). The transmission electron microscopy was carried out at the Virginia Tech Nanoscale Characterization and Fabrication Laboratory (ICTAS-NCFL) and the elemental analysis at the Penn State Energy and Environmental Laboratories (EESL). DMA thanks the following Penn State personnel: Mr. Matthew Gonzales (Penn State EESL) for extensive discussion of ICP-MS data and Ms. Rose Kerr (Penn State Behrend) for laboratory assistance. She thanks the following Virginia Tech faculty, students, and staff for assistance with instrumentation and laboratory space: Mr. Rui Serra Maia, Ms. Athena Tilley, Dr. Weinan Leng, Dr. Michael Hochella, and Dr. Marc Michel. She thanks Dr. Lisa Nogaj of Gannon University for providing access to an ultracentrifuge. She is grateful to Dr. William Casey (UC Davis) and Dr. Bernhard Peucker-Ehrenbrink (Woods Hole Oceanographic) for insightful discussions that inspired this research, and Dr. Adam Wallace (U

Delaware) for reviewing this paper. Finally, she thanks the two anonymous reviewers for suggestions that improved this paper significantly.

Table 1. Elemental analysis of ACC solids (μmol kg^{-1})

Analyte	Pd	Pt	Rh	Zr	Ce	Au
Concentration	49000	2000	4519	760765	124190	6.7
Detection limit	0.047	0.026	0.049	22	713	0.010

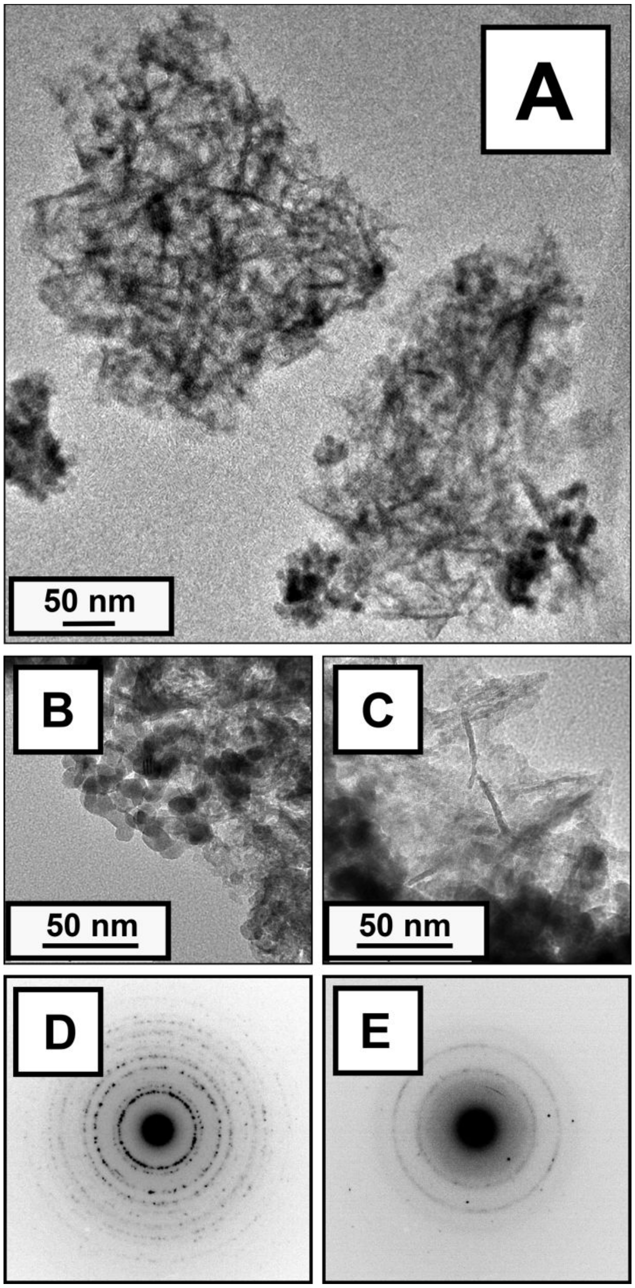

Figure 1. (a-c) Bright-field transmission electron microscopy (TEM) images of surface scrapings from VCC material: (a) Representative view of VCC materials; (b) Magnified image of nanodots; (c) Magnified image of nanoflakes. (d-e) Selected area electron diffraction (SAED): (d) SAED from nanodots, consistent with zirconia-ceria; (e) SAED

from lathe-like nanostructures consistent with γ-Al_2O_3. For indexing of these patterns, please see Tables S1 and S2 in the ESI.

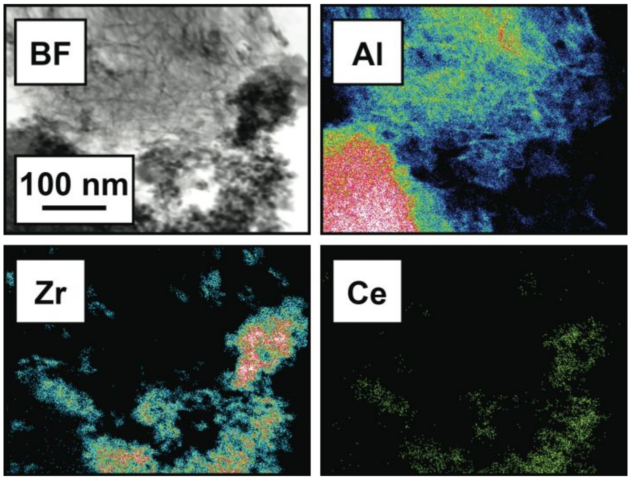

Figure 2. Bright-field TEM image and corresponding EDX elemental maps. The aluminum map displays more signal in the areas with the lathe-like structures, and the zirconium and cerium are localized to the dot-like structures.

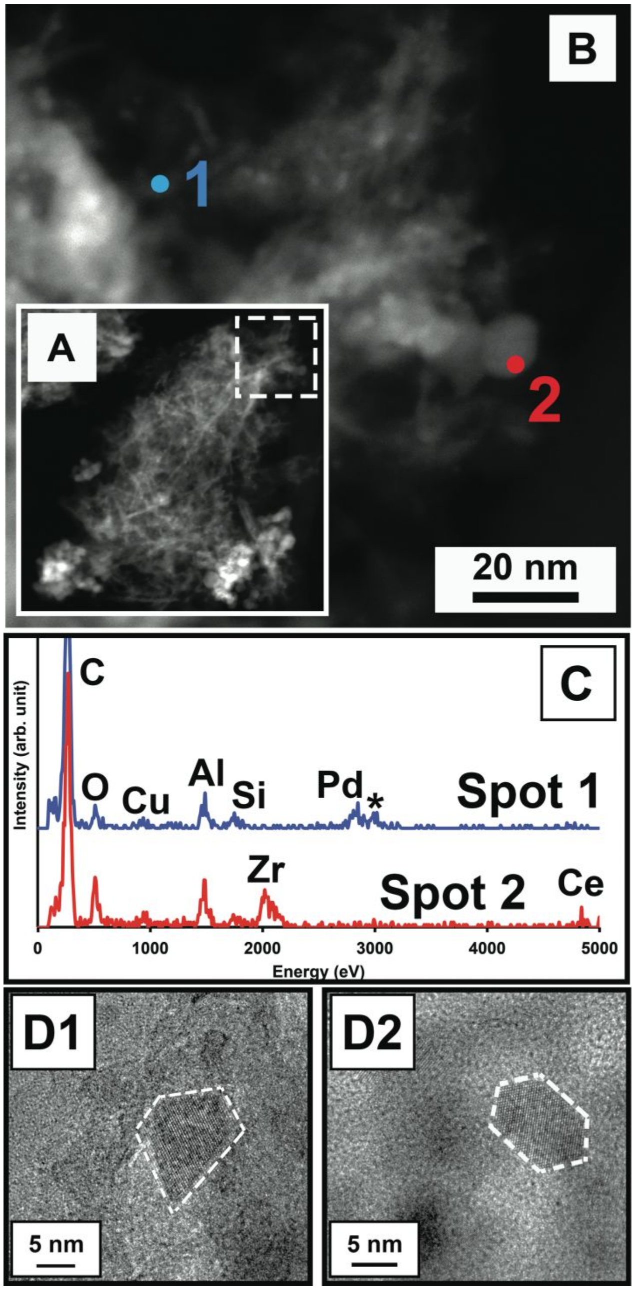

Figure 3. Localized chemical analysis and imaging of palladium-rich areas: (a) HAADF image of VCC material in Figure 1a; (b) Magnified section of dashed box area in (a). EDX sampling areas are marked; (c) EDX spectra from spots 1 and 2. The asterisk in the spot 1 spectrum corresponds to an Al-Al sum peak (2.972 eV); (d) HRTEM from

spot 1 area (EDX spectra indicate presence of palladium) with crystalline nanoparticles outlined.

Table 2.

Palladium concentrations (μM) in extracts from vehicle catalytic converter materials				
	No TAN*	Low TAN	Mid TAN	High** TAN
AN* only	0.010 (±0.005)	0.013 (±0.009)	0.059 (±0.040)	54.9 (±9.1)
AN + Cl^-	0.240 (±0.042)	0.253 (±0.103)	2.41 (±1.22)	75.5 (±14.7)

*Ammonia nitrogen (AN) refers to both species of ammonia, namely NH_3 and NH_4^+ (ammonium). Total ammonia nitrogen (TAN) is defined as $[NH_3] + [NH_4^+]$.

**Low refers to 5.56 μM TAN, mid refers to 55.6 μM TAN, and high refers to 1.13×10^5 μM TAN.

Table 3.

Platinum concentrations (μM) in extracts from vehicle catalytic converter materials			
No TAN*	Low TAN	Mid TAN	High** TAN

AN	1.90×10^{-4} ($\pm1.23\times10^{-4}$)	1.69×10^{-4} ($\pm0.051\times10^{-4}$)	2.36×10^{-4} ($\pm0.067\times10^{-4}$)	7.85×10^{-3} ($\pm3.64\times10^{-3}$)
AN + Cl^-	4.76×10^{-4} ($\pm1.33\times10^{-4}$)	6.87×10^{-4} ($\pm0.031\times10^{-4}$)	1.05×10^{-3} ($\pm0.034\times10^{-3}$)	8.41×10^{-3} ($\pm3.79\times10^{-3}$)

*Ammonia nitrogen (AN) refers to both species of ammonia, namely NH_3 and NH_4^+ (ammonium). Total ammonia nitrogen (TAN) is defined as $[NH_3] + [NH_4^+]$.

**Low refers to 5.56 µM TAN, mid refers to 55.6 µM TAN, and high refers to 1.13×10^5 µM TAN.

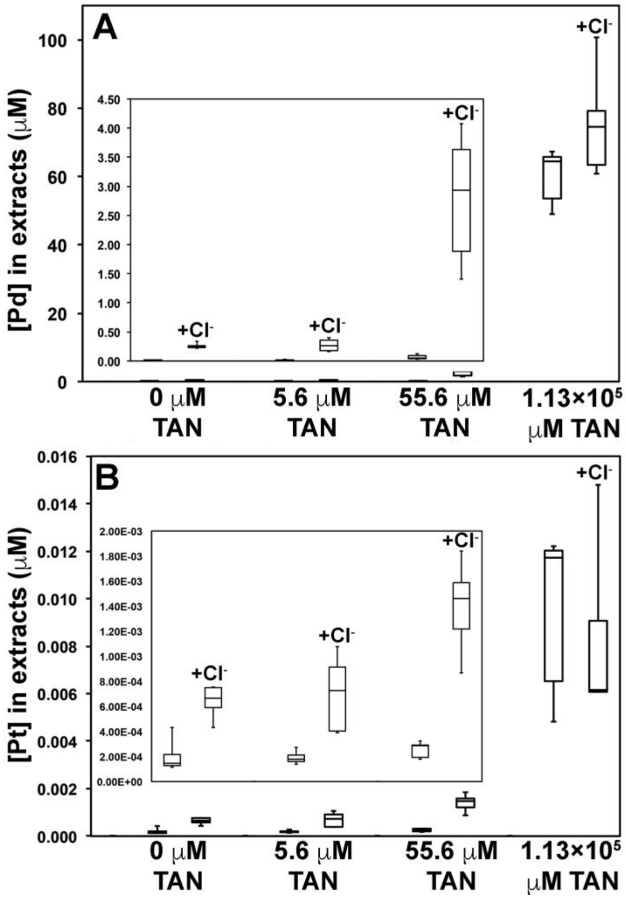

Figure 4. Box-and-whisker plots of Pd and Pt concentrations in extracts from VCC materials. Inset boxes show data for 0 μM, 5.56 μM (low TAN) and 55.6 μM (mid TAN) TAN solutions re-plotted on a smaller scale. Data from TAN-only solutions are paired with the corresponding TAN + Cl^- solution. (a) Palladium concentrations. (b) Platinum concentrations. See text and ESI for information on statistical analyses.

Notes and references

[‡]The terminology "total ammonia nitrogen (TAN)" is used in official US EPA documentation (see reference 51) and hence is used here for consistency. TAN specifically refers to the combined concentrations of unionized ammonia (NH_3) and ionized ammonia (NH_4^+ (ammonium)). "Ammonia nitrogen (AN)" is derived from this EPA terminology. It refers to both species of ammonia collectively.

1. C. Fortin, F. Wang and D. Pitre, *Critical Review of Platinum Group Elements (Pd, Pt, Rh) in Aquatic Ecosystems*, Environment Canada, 2011.
2. S. Rauch and G. M. Morrison, The Environmental Relevance of the Platinum Group Elements, *Elements*, 2008, **4**, 259-263.
3. F. Reith, S. G. Campbell, A. S. Ball, A. Pring and G. Southam, Platinum in Earth surface environments, *Earth-Science Reviews*, 2014, **131**, 1-21.
4. S. Rauch and B. Peucker-Ehrenbrink, in *Platinum Metals in the Environment*, ed. F. Z. a. C. L. S. Wiseman, Springer-Verlag, Berlin, Germany, 2015, pp. 3-17.
5. M. Moldovan, M. A. Palacios, M. M. Gomez, G. Morrison, S. Rauch, C. McLeod, R. Ma, S. Caroli, A. Alimonti, F. Petrucci, B. Bocca, P. Schramel, M. Zischka, C. Petterson, U. Wass, M. Luna, J. C. Saenz and J. Santamaria, Environmental Risk of Particulate and Soluble Platinum Group Elements Released from Gasoline and Diesel Engine Catalytic Converters., *Science of the Total Environment*, 2002, **296**, 199-208.
6. P. W. Ash, D. A. Boyd, T. I. Hyde, J. L. Keating, G. Randlshofer, K. Rothenbacher, G. Sankar, J. J. Schauer, M. M. Shafer and B. M. Toner, Local structure and speciation of platinum in fresh and road-aged North American sourced vehicle emissions catalysts: An X-ray absorption spectroscopic study, *Environmental Science and Technology*, 2014, **48**, 3568-3665.

7. A. Bozlaker, N. J. Spada, M. P. Fraser and S. Chellam, Elemental Characterization of PM2.5 and PM10 Emitted from Light Duty Vehicles in the Washburn Tunnel of Houston, Texas: Release of Rhodium, Palladium and Platinum, *Environmental Science and Technology*, 2014, **48**, 54-62.

8. F. Zereini, C. L. S. Wiseman and W. Püttmann, In Vitro Investigations of Platinum, Palladium and Rhodium Mobility in Urban Airborne Particulate Matter (PM10, PM2.5, and PM1) Using Simulated Lung Fluids. , *Environmental Science and Technology*, 2012, **46**, 10326-10333.

9. O. Morton-Bermea, O. Amador-Muñoz, L. Martínez-Trejo, E. Hernández-Álvarez, L. Beramendi-Orosco and M. E. García-Arreola, Platinum in PM2.5 of the metropolitan area of Mexico City., *Environmental Geochemistry and Health*, 2014, **36**, 987-994.

10. H. M. Prichard and P. C. Fisher, Identification of Platinum and Palladium Particles Emitted from Vehicles and Dispersed into the Surface Environment. , *Environmental Science and Technology*, 2012, **46**, 3149-3154.

11. H. Lee, H. Chon, M. Sager and L. Marton, Platinum pollution in road dusts, roadside soils, and tree barks in Seoul, Korea., *Environmental Geochemistry and Health*, 2012, **34**, 5-12.

12. T. Soyol-Erdene, Y. Huh, S. Hong and S. D. Hur, A 50-Year Record of Platinum, Iridium and Rhodium in Antarctic Snow: Volcanic and Anthropogenic Sources, *Environmental Science and Technology*, 2011, **45**, 5929-5935.

13. I. O. o. M. V. Manufacturers, Provisional Registrations or Sales of New Vehicles - All Types, http://www.oica.net/category/sales-statistics/).

14. I. O. o. M. V. Manufacturers, World Vehicles in Use - All Vehicles, http://www.oica.net/wp-content/uploads//Total_in-use-All-Vehicles.pdf).

15. I. S. Sen, Platinum Group Element Pollution is a Growing Concern in Countries with Developing Economy, *Environmental Science and Technology*, 2013, **47**, 13903-13904.

16. J. M. P. M. Management, *PGM Market Report May 2016*, Johnson Matthey, Royston, U.K., 2016.

17. L. Kelland, The Resurgence of Platinum-Based Cancer Chemotherapy, *Nature Reviews Cancer*, 2007, **7**, 573-584.

18. A. S. Abu-Surrah, H. H. Al-Sa'doni and M. Y. Abdalla, Palladium-based chemotherapeutic agents: Routes toward complexes with good antitumor activity, *Cancer Therapy*, 2008, **6**, 1-10.

19. C. K. Melber, D. Keller and I. Mangelsdorf, *Environmental Health Criteria 226: Palladium*, World Health Organization, 2002.

20. A. Garoufis, S. K. Hadjikakou, N. I. Hadjiliadis and C. L. S. Wiseman, in *Metallotherapeutic Drugs and Metal-Based Diagnostic Agents: The Use of Metals in Medicine*, ed. E. a. T. Gielen, R.T., Wiley, Hoboken, NJ, USA, 2005, pp. 399-419.

21. M. Shimizu and B. Rosenberg, SIMILAR ACTION TO UV-IRRADIATION AND A PREFERENTIAL INHIBITION OF DNA-SYNTHESIS IN ESCHERICHIA-COLI BY ANTITUMOR PLATINUM COMPOUNDS, *Journal of Antibiotics*, 1973, **26**, 243-245.

22. B. Rosenberg, L. Van Camp and T. Krigas, Inhibition of Cell Division in Escherichia coli by Electrolysis Products from a Platinum Electrode, *Nature* 1965, **205**, 698-699.

23. P. Sobrova, J. Zehnalek, V. Adam, M. Beklova and R. Kizek, The effects on soil/water/plant/animal systems by platinum group elements, *Central European Journal of Chemistry*, 2012, **10**, 1369-1382.

24. J. Malm and J. Bovin, High resolution electron microscopy of a used automobile catalytic converter, *Microscopy Microanalysis Microstructures*, 1990, **1**, 387-394.

25. D. M. Aruguete, J. Liu and M. F. Hochella Jr., in *Environmental and Human Health Impacts of Nanotechnology*, eds. J. R. Lead and E. Smith, Blackwell, Chippenham, Wiltshire, UK, 2009, ch. 3, pp. 79-108.

26. J. Liu, D. M. Aruguete, M. Murayama and M. F. Hochella Jr., Influence of Size and Aggregation on the Reactivity of an Environmentally and Industrially Relevant Nanomaterial, *Environmental Science and Technology*, 2009, **43**, 8178-8183.

27. M. Baalousha, Y. Yang, M. E. Vance, B. P. Colman, S. McNeal, J. Xu, J. Blaszczak, M. Steele, E. Bernhardt and M. F. Hochella Jr., Outdoor Urban Nanomaterials: The Emergence of a New, Integrated, and Critical Field of Study, *Science of the Total Environment*, 2016, **557-558**, 740-757.

28. F. Zereini, C. L. S. Wiseman, M. Vang, P. Albers, W. Schneider, R. Schindl and K. Leopold, Geochemical Behaviour of Palladium in Soils and Pd/PdO Model Substances in the Presence of the Organic Complexing Agents L-Methionine and Citric Acid. , *Environmental Science: Processes and Impacts*, 2016, **18**, 22-31.

29. S. Lustig, S. Zang, W. Beck and P. Schramel, Dissolution of metallic platinum as water soluble species by naturally occurring complexing agents, *Mikrochimica Acta*, 1998, **129**, 189-194.

30. V. Suchá, M. Mihaljevič, V. Ettler and L. Strnad, The pH-dependent release of platinum group elements (PGEs) from gasoline and diesel fuel catalysts: Implication for weathering in soils, *Journal of Environmental Management*, 2016, **171**, 52-59.

31. F. Zereini, I. Muller and C. L. S. Wiseman, in *Platinum Metals in the Environment*, eds. F. Zereini and C. L. S. Wiseman, Springer-Verlag, Berlin, Germany, 2015.

32. F. Zereini, C. L. S. Wiseman, J. Poprizki, P. Albers, W. Schneider and K. Leopold, Assessing the potential of inorganic anions (Cl-, NO3-, SO42- and PO43-)

to increase the bioaccessibility of emitted palladium in the environment: Experimental studies with soils and a Pd model substance, *Environmental Pollution*, 2017, **220**, 1050-1058.

33. A. Turner and S. Price, Bioaccessibility of Platinum Group Elements in Automotive Catalytic Converter Particulates., *Environmental Science and Technology*, 2008, **42**, 9443-9448.

34. J. O'M. Bockris and A. K. N. Reddy, in *Modern Electrochemistry 2: An Introduction to an Interdisciplinary Area*, Plenum Press, New York, NY, 1970, vol. 2, ch. 11, pp. 1265-1432.

35. H. Luo, S. Park, Y. H. Chan and M. J. Weaver, Surface oxidation of platinum-group transition metals in ambient gaseous environments: Role of electrochemical versus chemical pathways, *Journal of Physical Chemistry B*, 2000, **104**, 8250-8258.

36. N. N. Greenwood and A. Earnshaw, *Chemistry of the Elements*, Butterworth-Heinemann, Oxford, U.K., 2nd edn., 1997.

37. M. Azaroual, B. Romand, P. Freyssinet and J. Disnar, Solubility of platinum in aqueous solutions at 25°C and pHs 4 to 10 under oxidizing conditions, *Geochimica et Cosmochimica Acta*, 2001, **65**, 4453-4466.

38. S. A. Wood, B. W. Mountain and P. Pan, The Aqueous Geochemistry of Platinum, Palladium and Gold: Recent Experimental Constraints and a Reevaluation of Theoretical Predictions, *Canadian Mineralogist*, 1992, **30**, 955-982.

39. C. Colombo, C. J. Oates, A. J. Monhemius and J. A. Plant, Complexation of platinum, palladium and rhodium with inorganic ligands in the environment, *Geochemistry: Exploration, Environment, Analysis*, 2008, **8**, 1-11.

40. C. H. Gammons, Experimental investigations of the hydrothermal geochemistry of platinum and palladium: V. Equilibria between platinum metal, Pt(II), and Pt (IV) chloride complexes at 25 to 300°C, *Geochimica et Cosmochimica Acta*, 1996, **60**, 1683-1694.

41. J. M. Van Middlesworth and S. A. Wood, The stability of palladium(II) hydroxide and hydroxy-chloride complexes: An experimental solubility study at 25-85° C and 1 bar, *Geochimica et Cosmochimica Acta*, 1999, **63**, 1751-1765.

42. P. P. Lopes, D. Strmcnik, D. Tripkovic, J. G. Connell, V. Stamenkovic and N. M. Markovic, Relationships between Atomic Level Surface Structure and Stability/Activity of Platinum Surface Atoms in Aqueous Environments, *ACS Catalysis*, 2016, **6**, 2536-2544.

43. F. Basolo, in *Mechanisms of Inorganic Reactions*, ed. J. M. Kleinberg, R.K.; Fraser, R.T.M.; Bauman, J., American Chemical Society, Washington, D.C., USA, 1965, pp. 81-106.

44. A. Kitamura, R. Doi and Y. Yoshida, *Update of JAEA-TDB Update of thermodynamic data for palladium and tin, refinement of thermodynamic data for protactinium, and preparation of PHREEQC database for use of the Brønsted-Guggenheim-Scatchard model*, Japan Atomic Energy Agency, Japan, 2014.

45. A. E. Martell and R. M. Smith, *Critical Stability Constants: Inorganic Complexes*, Springer US, New York, NY, 1976.

46. L. I. Elding, STABILITIES OF PLATINUM(II) CHLORO AND BROMO COMPLEXES AND KINETICS FOR ANATION OF TETRAAQUAPLATINUM(II)

ION BY HALIDES AND THIOCYANATE, *Inorganica Chimica Acta*, 1978, **28**, 255-262.

47. R. Sefako, K. Sekgarametso and V. Sibanda, Potential Processing Routes for Recovery of Platinum Group Metals from Southern African Oxidized PGM Ores: A Review, *Journal of Sustainable Metallurgy*, 2017, **3**, 797-807.

48. F. L. Bernardis, R. A. Grant and D. C. Sherrington, A review of methods of separation of the platinum-group metals through their chloro-complexes, *Reactive & Functional Polymers*, 2005, **65**, 205-217.

49. A. F. S. Gouldsmith and B. Wilson, Extraction and Refining of the Platinum Metals: A Complex Cycle of Smelting, Electrolytic and Chemical Operations, *Platinum Metals Review*, 1963, **7**, 136-143.

50. R. G. Bates and G. D. Pinching, Acidic Dissociation Constant of Ammonium Ion at 0° to 500° C, and the Base Strength of Ammonia
, *Journal of Research of the National Bureau of Standards*, 1949, **42**, 419-430.

51. M. A. Sutton, J. W. Erisman, F. Dentener and D. Moller, Ammonia in the environment: From ancient times to the present, *Environmental Pollution*, 2008, **156**, 583-604.

52. N. Roney, F. Llados, S. S. Little and D. B. Knaebel, Toxicological Profile for Ammonia.*Journal*, 2004.

53. U. S. E. P. Agency, *Aquatic Life Ambient Water Quality Criteria for Ammonia – Freshwater (EPA 822-R-13-001)*, U.S. Environmental Protection Agency, Washington, D.C. U.S., 2013.

54. J. Li and R. H. Byrne, Amino acid complexation of palladium in seawater, *Environmental Science and Technology*, 1990, **24**, 1038-1041.

55. A. Singh, Managing the salinization and drainage problems of irrigated areas through remote sensing and GIS techniques, *Ecological Indicators*, 2018, **89**, 584-589.

56. V. Re and E. Sacchi, Tackling the salinity-pollution nexus in coastal aquifers from arid regions using nitrate and boron isotopes, *Environmental Science and Pollution Research*, 2017, **24**, 13247-13261.

57. C. Amrhein, J. E. Strong and P. A. Mosher, Effect of Deicing Salts on Metal and Organic Matter Mobilization in Roadside Soils, *Environmental Science and Technology*, 1992, **26**, 703-709.

58. S. R. Corsi, D. J. Graczyk, S. W. Geis, N. L. Booth and K. D. Richards, A Fresh Look at Road Salt: Aquatic Toxicity and Water-Quality Impacts on Local, Regional and National Scales, *Environmental Science and Technology*, 2010, **44**, 7376-7382.

59. K. V.R., F. S.E., W. H. Schlesinger, K. Menking and A. M. Chatrchyan, *Road Salt: Moving Towards the Solution.*, Cary Institute of Ecosystem Studies, Millbrook, NY, 2010.

60. J. R. Mullaney, D. L. Lorenz and A. D. Arntson, *Chloride in Groundwater and Surface Water in Areas Underlain by the Glacial Aquifer System, Northern United States*, U.S. Geological Survey, Reston, VA, USA, 2009.

61. F. G. Renaud, T. T. H. Le, C. Lindener, V. T. Guong and Z. Sebesvari, Resilience and shifts in agro-ecosystems facing increasing sea-level rise and salinity intrusion in Ben Tre Province, Mekong Delta., *Climatic Change*, 2015, **133**, 69-84.

62. W. Liu and H. Liu, Assessing the Impacts of Sea Level Rise on Salinity Intrusion and Transport Time Scales in a Tidal Estuary, Taiwan, *Water*, 2014, **6**, 324-344.

63. E. C. H. Canada, *Priority Substance List Assessment Report – Road Salt*, Environment Canada Health Canada, Ottawa, ON, Canada, 2001.

64. R. L. Ohrel Jr. and K. M. Register, Volunteer Estuary Monitoring: A Methods Manual, Second Edition.*Journal*, 2006, 14-11 - 14-18.

65. in *Standard Methods for the Examination of Water and Wastewater*, eds. E. W. Rice, R. B. Baird, A. D. Eaton and L. S. Clesceri, American Public Health Association, Washington, DC, USA, 22nd edn., 2012.

66. L. Guo and P. H. Santschi, in *Environmental Colloids and Particles: Behaviour, Separation and Characterization*, ed. K. J. W. Jamie R. Lead, IUPAC, 2007, ch. 4, pp. 159-221.

67. A. Shrivastava and V. B. Gupta, Methods for the determination of limit of detection and limit of quantitation of the analytical methods, *Chronicles of Young Scientists*, 2011, **2**, 21-25.

68. V. S. L. Escribano, E.F.; Panizza, M.; Resini, C., Amores, J.M.G. and Busca, G. , Characterization of cubic ceria-zirconia powders by X-ray diffraction and vibrational and electronic spectroscopy, *Solid State Science*, 2003, **5**, 1369-1376.

69. M. Trueba and S. P. Trasatti, γ-Alumina as a Support for Catalysts: A Review of Fundamental Aspects, *European Journal of Inorganic Chemistry*, 2005, 3393-3403.

70. P. Vaný́sek, in *CRC Handbook of Chemistry and Physics*, ed. D. Lide, CRC Press, Boca Raton, FL, U.S.A., 89th edn., 2008, ch. 8, pp. 20-29.

71. A. A. El-Sherif, in *Stoichiometry and Research: The Importance of Quantity in Biomedicine*, ed. A. Innocenti, IntechOpen, 2012.

72. K. Folens, T. Van Acker, E. Bolea-Fernandez, G. Cornelis, F. Vanhaecke, G. Du Laing and S. Rauch, Identification of platinum nanoparticles in road dust leachate

by single particle inductively coupled plasma mass spectrometry, *Science of the Total Environment*, 2018, **615**, 849-856.

73. S. A. Wood and B. W. Mountain, Thermodynamic constraints on the solubility of platinum and palladium in hydrothermal solutions: Reassessment of hydroxide, bisulfide, and ammonia complexing, *Economic Geology*, 1989, **84**, 2020-2028.

74. J. M. Cosden and R. H. Byrne, Comparative geochemistries of Pd(II) and Pt(II): Formation of mixed hydroxychloro and chlorocarbonato-complexes in seawater, *Geochimica et Cosmochimica Acta*, 2003, **67**, 1331-1338.

75. R. A. Reinhardt, N. L. Brenner and R. K. Sparkes, EQUILIBRIA AMONG CHLOROAMMINE COMPLEXES OF PALLADIUM(2), *Inorganic Chemistry*, 1967, **6**, 254-+.

76. R. A. Reinhardt, *Equilibrium and kinetics of some simple complexes of palladium(II)*, Naval Postgraduate Academy, 1976.

77. R. A. Reinhardt and R. K. Sparkes, KINETICS OF CONSECUTIVE SUBSTITUTIONS OF AMMONIA BY CHLORIDE ION IN TETRAAMMINEPALLADIUM(2) ION, *Inorganic Chemistry*, 1967, **6**, 2190-+.

78. R. A. Reinhardt and W. W. Monk, KINETICS OF SUCCESSIVE AMMONATION REACTIONS OF TETRACHLOROPALLADATE(II) ION, *Inorganic Chemistry*, 1970, **9**, 2026-&.

79. L. I. Elding and L. F. Olsson, ELECTRONIC ABSORPTION-SPECTRA OF SQUARE-PLANAR CHLORO-AQUA AND BROMO-AQUA COMPLEXES OF PALLADIUM(II) AND PLATINUM(II), *Journal of Physical Chemistry*, 1978, **82**, 69-74.

80. T. S. Shi and L. I. Elding, Equilibria, kinetics and mechanism for complex formation between hydrogen sulfate/sulfate and palladium(II). Hydrolysis of tetraaquapalladium(II), *Acta Chemica Scandinavica*, 1998, **52**, 897-902.

81. L. I. Elding and L. Gustafson, KINETICS AND MECHANISM FOR CHLORIDE ANATION OF SOME PLATINUM(IV) AQUA COMPLEXES IN PRESENCE OF PLATINUM(II), *Inorganica Chimica Acta*, 1976, **19**, 31-38.

82. L. I. Elding, KINETICS FOR ANATION OF AQUA PALLADATE(II) COMPLEXES, *Inorganica Chimica Acta*, 1975, **15**, L9-L11.

83. L. I. Elding and A. B. Groning, LIGAND SUBSTITUTION-REACTIONS OF MIXED CHLORO-BROMO COMPLEXES OF PLATINUM(II) - EQUILIBRIA, KINETICS, AND MECHANISM, *Chemica Scripta*, 1977, **11**, 8-16.

84. L. Drougge and L. I. Elding, MECHANISMS FOR ACCELERATION OF HALIDE ANATION REACTIONS OF PLATINUM(IV) COMPLEXES - REOA VERSUS LIGAND ASSISTANCE AND PLATINUM(II) CATALYSIS WITHOUT CENTRAL ION-EXCHANGE, *Inorganica Chimica Acta*, 1986, **121**, 175-183.

85. L. I. Elding and I. Leden, On the Stepwise Dissolution of the Tetrachloridoplatinate(II) Ion in Aqueous Solution. I. Equilbria at 25 C., *Acta Chemica Scandinavica*, 1966, **20**, 706-715.

86. L. I. Elding and L. Gustafson, RATES AND MECHANISMS FOR HALIDE ANATION REACTIONS OF PLATINUM(IV) COMPLEXES, *Inorganica Chimica Acta*, 1977, **24**, 239-246.

87. L. I. Elding, STEPWISE DISSOCIATION OF TETRACHLORIDOPLATINATE(2) ION IN AQUEOUS SOLUTION .2. KINETICS OF FIRST STEP, *Acta Chemica Scandinavica*, 1966, **20**, 2559-&.

88. L. I. Elding, STEPWISE DISSOCIATION OF TETRACHLOROPLATINATE(II) ION IN AQUEOUS SOLUTION .5. CHLORIDE ANATIONS OF CHLORO AQUA COMPLEXES OF PLATINUM(II), *Acta Chemica Scandinavica*, 1970, **24**, 1341-&.

89. L. I. Elding, STEPWISE DISSOCIATION OF TETRACHLOROPLATINATE(II) ION IN AQUEOUS SOLUTION .6. RATES OF FORMATION AND EQUILIBRIA

OF CHLORO AQUA COMPLEXES OF PLATINUM(II), *Acta Chemica Scandinavica*, 1970, **24**, 1527-&.

90. L. Drougge, L. I. Elding and L. Gustafson, Stepwise Dissociation of the Tetrachloroplatinate(II) Ion in Aqueous Solution III. Influenced of Temperature and Kinetics and Equilibrium of the First Step, *Acta Chemica Scandinavica*, 1967, **21**, 1647-1653.

91. J. J. Cruywagen and R. J. Kriek, Complexation of palladium(II) with chloride and hydroxide, *Journal of Coordination Chemistry*, 2007, **60**, 439-447.

92. L. I. Elding, Palladium(II) halide complexes. II. Acid hydrolysis and halide anations of palladium(II) chloro and bromo aqua complexes., *Inorganica Chimica Acta*, 1972, **6**.

Table of Contents Entry

For “Enhanced release of palladium and platinum from catalytic converter materials exposed to ammonia and chloride bearing solutions”

Authors and affiliations:

Deborah M. Aruguete[1]*, Mitsuhiro Murayama[2,3], Terry Blakney[4] and Christopher Winkler[3]

[1]Department of Environmental Science, Penn State Behrend, 4205 College Drive, Erie, PA 16563, U.S.A.

[2]Department of Materials Science and Engineering, Virginia Tech, Blacksburg, VA, 24061, U.S.A.

[3]Institute for Critical Technology and Applied Science, Nanoscale Characterization and Fabrication Laboratory, Virginia Tech, Blacksburg, VA, 24061, U.S.A

[4]Department of Mathematics, Penn State Behrend, 4205 College Drive, Erie, PA 16563

*Corresponding author: aruguete@psu.edu

Table of Contents Entry

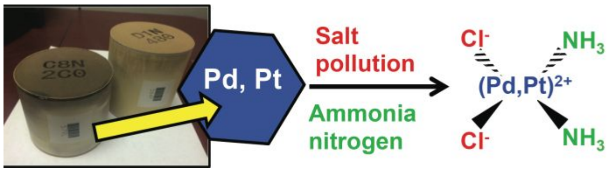

Results suggest systems with elevated salinity and trace ammonia could induce release of palladium/platinum from emitted vehicle catalytic converter (VCC) materials; electron microscopy suggests presence of non-metallic palladium in VCCs.